Integration of Simple Antennas to Multiband Receivers using a Novel Multiplexer Design Methodology

S.M. Shajedul Hasan and S.W. Ellingson

This is a preprint of a paper accepted by the IEEE Trans. Antennas and Propagation.
© 2011 IEEE

The published version of this paper is:
S.M.S. Hasan & S.W. Ellingson, "Integration of Simple Antennas to Multiband Receivers using a Novel Multiplexer Design Methodology", *IEEE Trans. Ant. & Prop.*, Vol. 60, No. 3, March 2012, pp. 1550-6.
http://dx.doi.org/10.1109/TAP.2011.2180309

Integration of Simple Antennas to Multiband Receivers using a Novel Multiplexer Design Methodology

S.M. Shajedul Hasan, *Member, IEEE,* and Steven W. Ellingson, *Senior Member, IEEE*

***Abstract*—This paper presents a new concept in RF multiplexer design to integrate a single monopole–type antenna to a receiver with large, multiband tuning ranges. Traditional techniques to integrate a single antenna with such receivers are limited in their ability to handle simultaneous channels distributed over very large tuning ranges, which is important for frequency-agile cognitive radio, surveillance, and other applications requiring wideband or multiband monitoring. In our approach, the goal is first to achieve sensitivity which is nominally dominated by external (environmental) noise, and then secondly to improve bandwidth to the maximum possible consistent with this goal. A procedure is described for designing antenna–multiplexer–preamplifier assemblies using this philosophy. It is shown that the approach can significantly increase the usable bandwidth and number of bands that can be supported by a single, traditional antenna. A three channel (10–28 MHz, 32–50 MHz, and 54–80 MHz) multiplexer for a VHF monopole antenna was designed and performance was validated through field experiment.**

***Index Terms*—Multiband Antenna, Mobile Radio Antenna, Antenna Matching, Multiplexer, Antenna Integration, VHF Band, UHF Band, Multiband Receiver.**

I. Introduction

Commercial, military, and public safety operations use mobile and portable radio at HF (25–30 MHz); VHF (30–50, 138–174, and 220–222 MHz); and UHF (406–512 MHz, and segments between 700 MHz and 1000 MHz) frequencies. Traditionally, radios designed for these applications are able to use just one or two of these bands. In recent years, however, desire for improved communications interoperability, combined with improvements in radio electronics, have led to a new generation of multiband radios (MBRs) which are capable of operating in many of these bands. In particular, some currently–available MBRs advertise tuning ranges of 30–512 MHz for military applications and 136–870 MHz for public safety applications. Although detailed specifications for new MBRs are typically not publicly available, it is known that these radios require antenna changes to achieve acceptable sensitivity over the entire tuning range. This is because it is very difficult to design a single monopole–type antenna which performs well in many bands, especially when each band has relatively large fractional bandwidth. Solutions which eliminate the need to switch antennas, or which allow existing antennas to be effective over a larger range of frequencies, are of great interest.

S.M. Shajedul Hasan and S.W. Ellingson are with the Bradley Department of Electrical and Computer Engineering, Virginia Tech, Blacksburg, VA 24061, USA, e-mails: hasan@vt.edu, ellingson@vt.edu.

Manuscript received XXXX XX, 2010; revised XXXX XX, 2011.

Potential solutions to this problem include broadbanding the antenna, active matching, and non–Foster matching. Broadbanding the antenna inevitably requires modifications to the geometry, such as wire thickening or "top hatting", that users typically find unacceptable. Active matching – that is, dynamically tuning the antenna match as the radio is tuned – inevitably results in a reduction of instantaneous bandwidth, which constrains the ability of the radio to scan and monitor other channels. Non-Foster matching is a potential future solution, but currently suffers from limitations in linearity and noise figure which make it unsuitable for most applications [1].

In this paper we consider an alternative approach in which the antenna is interfaced to the radio using a multiplexer. Traditionally, antenna multiplexers (or multicouplers, as they are sometimes known), are used simply to channelize the antenna output into multiple bands, where each band is serviced by a different radio input. In our approach, the multiplexer is also used as a matching device; in particular (and unlike traditional multiplexers) the impedance of the common port is not constrained to be a standard value which is desired to be invariant with frequency. This has only very recently begun to be considered in the context of multiplexer design; for example, see [2]. A second difference in our approach is that the efficiency of the low-frequency channels of the multiplexer is intentionally sacrificed to obtain improved fractional bandwidth of the low-frequency channels, and improved efficiency of the high-frequency channels. This turns out to be particularly effective in the HF and VHF bands, where high external noise levels make efficiency less important, as will be explained in this paper. However, because transmit–mode performance depends directly on efficiency, this approach will only be suitable for receive–only or push–to–talk type systems.

The multiplexer approach turns out also to be particularly well-suited to the emerging generation of CMOS-based multiband radio-frequency integrated circuits (RFICs), for which this channelization is required to achieve selectivity requirements anyway (for example, see [3]). The fact that this approach results in multiple (frequency-partitioned) outputs is not a problem even for receiver systems consisting of a single input, since the multiplexer outputs are at a standard impedance and can be combined using traditional techniques. Disadvantages of this approach include the need for front-end amplifiers with relatively low-noise and high linearity, and the need for a separate traditional transmit path. We quantify the requirements for the former; the latter is only a minor issue especially for "push-to-talk" systems of the type identified

above.

In this paper, we explain the concept, present a design methodology, and provide a field demonstration. In the field demonstration, we show that a simple 36 MHz-resonant quarter-wave monopole connected to a custom three-channel passive multiplexer and followed by a front-end amplifier with 3 dB noise figure is able to achieve Celestial noise-limited (that is, the best possible) sensitivity in the ranges 10–28, 32–50, and 54–80 MHz simultaneously.

This paper is organized as follows. Section II describes the theory, including a system model to calculate the performance of RF multiplexers. Section III presents the multiplexer design methodology. The proposed concept is validated through a field experiment in Section IV. Finally, Section V summarizes this paper and presents some topics for future research.

II. Theory

Figure 1 shows the system model used to calculate the performance of our proposed multiplexer design methodology. This model consists of an antenna, a multiplexer, and a preamplifier. The power spectral density (PSD) delivered by the antenna into a matched load is

$$S_A = \eta k T_A \tag{1}$$

where η is efficiency associated with the loss due to the absorption by the imperfect (nonperfectly-conducting) ground, k is Boltzmann's constant (1.38×10^{-23} J/K), and T_A is antenna temperature. When no multiplexer is used, we have

$$S_{out}^{(1)} = S_A \left(1 - \left|\Gamma_A^{(1)}\right|^2\right) G_P + k T_P G_P \tag{2}$$

where $\Gamma_A^{(1)}$ in this case (no multiplexer in Figure 1) is Γ_P, i.e., the reflection coefficient at the interface of antenna and the preamplifier; T_P is the noise temperature of the preamplifier; and G_P is the total gain of the preamplifier. An estimate of S_A is therefore given by

$$\hat{S}_A = \frac{S_{out}^{(1)} - k T_P G_P}{\left(1 - \left|\Gamma_A^{(1)}\right|^2\right) G_P} \quad . \tag{3}$$

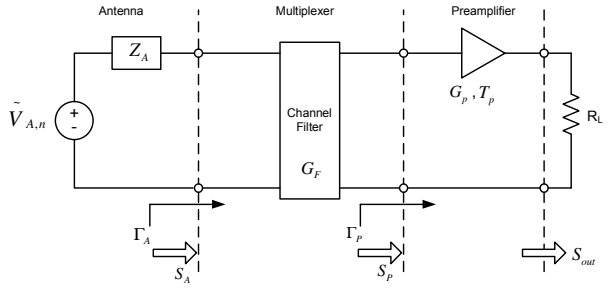

Fig. 1. System model to calculate the performance of multiplexer. The output impedance of the preamplifier is R_L

When the multiplexer is included, we have

$$S_{out}^{(2)} = S_P^{(2)} G_P + k T_P G_P \quad . \tag{4}$$

Now the PSD $S_P^{(2)}$ delivered to the preamplifier by the multiplexer channel can be estimated as

$$\hat{S}_P^{(2)} = \frac{S_{out}^{(2)} - k T_P G_P}{G_P} \quad . \tag{5}$$

In this paper, we use a performance metric known as transducer power gain (TPG) to characterize the performance of the multiplexer, specifically the efficiency of power transfer from antenna to the input of the receiver. TPG is defined as the ratio of power delivered by a matching network to the rest of the receiver, to the power delivered to a matched load attached directly to the antenna [4]. Combining Equations 3 and 5, the TPG of the multiplexer can be calculated from measurements of $S_{out}^{(1)}$ and $S_{out}^{(2)}$ as

$$\text{TPG} = \frac{\hat{S}_P^{(2)}}{\hat{S}_A} = \frac{S_{out}^{(2)} - k T_P G_P}{S_{out}^{(1)} - k T_P G_P} \left(1 - \left|\Gamma_A^{(1)}\right|^2\right) \quad . \tag{6}$$

The ratio of external noise to internally–generated noise is

$$\gamma = \eta \frac{T_A}{T_p} \left[1 - |\Gamma_A|^2\right] G_F \quad . \tag{7}$$

Both natural and man-made noise can be described in terms of a noise temperature T_A, following a power law af^{-b} where f is frequency, and variance with respect to location σ^2. The total noise temperature is the linear sum of the celestial noise and the applicable category of man-made noise. Values of a and b have been summarized in Table I, derived from data provided in [5].

The ratio of external noise to internally–generated noise was shown in the Equation 7. Clearly, sensitivity is optimized by minimizing $|\Gamma_A|$ (i.e., good matching) and minimizing T_p (i.e., low noise design). However, once γ is high the external (unavoidable) noise is dominating, so that additional effort to minimize $|\Gamma_A|$ or T_p will have little effect on sensitivity. Furthermore, if acceptable γ can be achieved for a poor $|\Gamma_A|$ – as is possible when T_A is large – improvements in $|\Gamma_A|$ are actually counter-productive, since this limits the design by imposing unnecessarily strict matching requirements.

This principle has already been demonstrated to be effective in the design of active antennas (see for example [6]); here we extend the concept using multiplexers as a means to obtain multiple broad tuning ranges.

III. Design Methodology

Our proposed technique starts with designing each of the multiplexer channel filters for standard (e.g., 50Ω) input and output impedance, connecting the input port of the multiplexer channels in parallel, and then performing an optimization of the multiplexer channels according to the following principles: (1) The ratio γ should be large, and (2) The multiplexer channel TPG should be "reasonably flat" over the passband.

Let the TPG of the channels be $T_i(\omega)$, where $i = 1, 2, \ldots, n$ represents the channel number; and the value of components (i.e., inductors or capacitors) used in the channels is represented by $X_{i,j}$, where $j = 1, 2, \ldots, p$ represents the component indexes within each channel. The optimization is

$$\min_{\{X_{i,j}\}} \quad \sum_{i=1}^{n} \int_{\omega_{a,i}}^{\omega_{b,i}} \left[T_i(\omega) - T_{BF,i}\right]^2 d\omega \tag{8}$$

TABLE I
PARAMETERS FOR NOISE TEMPERATURE $T_A = af^{-b}$ [K].

Frequency (MHz)		Quiet Rural	Rural	Residential	Business A/B	Celestial[1]
3–30	a	9.53×10^{24}	6.33×10^{25}	2.14×10^{26}	5.75×10^{26}	1.07×10^{23}
	b	2.86	2.77	2.77	2.77	2.52
30–100	a	–	6.33×10^{25}	2.14×10^{26}	5.75×10^{26}	1.07×10^{23}
	b	–	2.77	2.77	2.77	2.52
100–130	a	–	6.33×10^{25}	2.14×10^{26}	5.75×10^{26}	1.07×10^{23}
	b	–	2.77	2.77	2.77	2.52
130–250	a	–	6.33×10^{25}	2.14×10^{26}	1.87×10^{14}	1.07×10^{23}
	b	–	2.77	2.77	1.23	2.52
250–900	a	–	–	–	1.87×10^{14}	1.07×10^{23}
	b	–	–	–	1.23	2.52
900–3000	a	–	–	–	–	1.07×10^{23}
	b	–	–	–	–	2.52
σ		5.3 dB	5.3 dB	4.5 dB	6.6 dB	–

[1]Add 2.7 K to account for cosmic microwave background (CMB) radiation. Varies over about 2 dB depending on time of day; see [6].

where $T_{BF,i}$ is the theoretical TPG calculated using the Bode–Fano bound [7] at the center frequency of each channel; and $\omega_{a,i}$ and $\omega_{b,i}$ are the lower and higher cutoff frequencies of each channel respectively. This attempts to find $X_{i,j}$'s such that the best possible fit to the optimum estimated per–channel TPGs is obtained. Note that the quality of the fit is assessed using a mean–square error criteria. Since it is likely that a perfect solution will not be found, we also specify a criteria for stopping the optimization:

$$T_i(\omega)|_{max} - T_i(\omega)|_{min} < \epsilon_i \tag{9}$$

where $T_i(\omega)|_{max}$ and $T_i(\omega)|_{min}$ are the maximum and minimum values of the TPG over channel i, and ϵ_i is a "flatness" constraint for each channel. If the optimization does not converge as desired, the value of ϵ_i can be increased. Any multivariable optimization technique can be used to optimize the component values. The optimization does not require or depend on any particular algorithm. However, in this paper we used the simulation software GENESYS from Agilent Technologies[2], which uses the "pattern search" algorithm described in [8], to perform our optimization. In this optimization technique, each set of component values results in an error from the desired response. The error computed by GENESYS depends on which optimization method we use. The root mean square of individual parameter error terms is one approach. The error is then given by

$$E = \sqrt{\sum_n ((T_n - V_n)W_n)^p} \tag{10}$$

where p is error function power (always 2 or 6), T_n is set of target values (TPGs of the channels), V_n is set of actual values (theoretical TPGs), and W_n is set of target weights. The exponent "p" is always even, therefore the magnitude of each error contribution is always positive. In our case, since we are using pattern search,"p" is 2, which results in a root-mean-squared error minimization. Each target adds to the error value as determined by the above equation. A specified parameter has a default weight of 1 unless modified by the weight option. The optimization routine attempts to reduce the total error value by adjusting the values of all components listed in the variables list of the optimization properties. Optimization continues until the error reaches zero or close to zero. This design methodology is demonstrated in the next section.

[2]http://eesof.tm.agilent.com/products/genesys

IV. VHF–BAND MULTIPLEXER EXAMPLE

In this section we demonstrate the method and evaluate the design in field conditions. In this design example, we add a three–channel multiplexer to a VHF monopole antenna. A block diagram of the design is shown in Figure 2. A VHF monopole antenna is used in this experiment because monopole antennas are simple to design, and easy to analyze and build. Also relevant is the fact that antennas used in mobile and portable radios are more similar to monopoles than to dipoles.

A. Antenna and Multiplexer Design

We used a copper pipe 1.97 m long and 21 mm in diameter as our VHF monopole antenna. Since the Earth is not a perfect ground, a ground screen made from Reflectix brand foil insulation[3], which consists of two layers of aluminum foil with plastic bubble laminated between the foil layers (mostly used for thermal insulation) is used as for the ground screen for this experiment. Commercial software FEKO[4], which simulates an antenna using the Method of Moments (MoM), is used to model this antenna as copper wire of circular cross section. In our simulation, the ground screen is included above the Earth ground, which is assumed to have conductivity $\sigma = 5 \times 10^{-3}$ S/m and relative permittivity $\epsilon_r = 13$. From this we obtain the antenna self–impedance, needed to calculate reflection coefficients. The directivity and self-impedance of monopole antennas in the HF and VHF bands are well documented; see e.g. [9].

Our goal is to interface the antenna described above to separate receiver inputs corresponding to the 10-28 MHz, 32-50 MHz, and 54-80 MHz bands. We initially design the

[3]Model#ST16025, http://www.reflectixinc.com
[4]http://www.feko.info

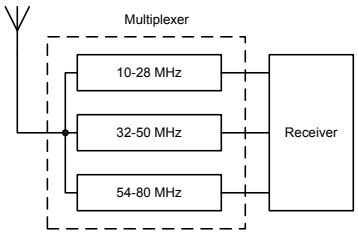

Fig. 2. VHF band multiplexer example.

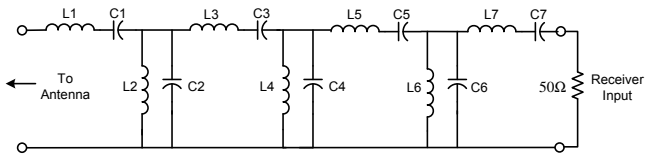

Fig. 3. Circuit topology of each multiplexer channel. The inputs of the three channels are connected in parallel.

multiplexer channels for constant 50Ω frequency–independent input and output impedances, neglecting the possibility of channel–to–channel interaction. Each of the channels of this multiplexer are designed using the 7^{th} order Chebyshev topology shown in Figure 3. Figure 4 shows the performance of this initial multiplexer assuming constant 50Ω antenna impedance. Once interfaced to the antenna, however, the result is as shown in Figure 5 (dotted lines). Note that the performance is dramatically degraded, especially in the 10–28 MHz band.

Before starting the optimization we need to have an idea about the theoretically best possible TPG, i.e., $T_{BF,i}$ for each multiplexer channel. The procedure of calculating this has been discussed elaborately in [10]. To calculate $T_{BF,i}$, the antenna impedance is approximated using a series RC or series RL model in each band. The procedure is specifically as follows: (1) For each channel's geometric center frequency (f_0), the impedance of the VHF monopole antenna is calculated; (2) From this impedance we calculate the value of the series resistance R, and the series capacitance C or series inductance L (depending on the positive or negative reactance value); (3) Using these values and the fractional bandwidths of each channel, the theoretical TPG is given by the following equations [11]:

$$\int_{-\infty}^{+\infty} \omega^{-2} \ln \left| \frac{1}{\Gamma(\omega)} \right| d\omega \leq \pi RC \qquad \text{(Series RC)} \qquad (11)$$

$$\int_{-\infty}^{+\infty} \omega \ln \left| \frac{1}{\Gamma(\omega)} \right| d\omega \leq \frac{\pi R}{L} \qquad \text{(Series RL)} \qquad (12)$$

and the resulting minimum possible refection coefficient Γ_{min}s are

$$\Gamma_{min} = \exp\left(-\frac{\pi RC\omega_0}{\mathrm{B}}\right) \qquad \text{(Series RC)} \qquad (13)$$

$$\Gamma_{min} = \exp\left(-\frac{\pi R}{L\omega_0 B}\right) \qquad \text{(Series RL).} \qquad (14)$$

where B will be $\omega_{b,i} - \omega_{a,i}$ for each channel i. Although the above bounds are useful to know the maximum achievable bandwidth given a TPG constraint, in reality it is not reasonable to specify a matching circuit with an infinite number of circuit components as is assumed in Equations 11–14. Fano obtained a modified version of the relationship presented above for a matching circuit using a n^{th} order Chebyshev topology [7], and finds

$$\Gamma_{min} = \frac{\cosh nb}{\cosh na} \qquad (15)$$

where the values of a and b can be calculated as follows [11]

$$a = \sinh^{-1}\left[\delta\left(1.7\delta^{-0.6} + 1\right)\sin\frac{\pi}{2n}\right] \qquad (16)$$

$$b = \sinh^{-1}\left[\delta\left(1.7\delta^{-0.6} - 1\right)\sin\frac{\pi}{2n}\right] \qquad (17)$$

where the parameter $\delta = 1/(BQ_L)$, and Q_L is defined as

$$Q_L = \frac{|X_s|}{R_s} = \frac{R_p}{|X_p|} \qquad (18)$$

where the impedance to be matched (i.e., Z_L) is represented as R_s and X_s connected in series, or R_p and X_p connected in parallel, and B is the fractional bandwidth in this case. Detail procedure of this can be found in [10].

The results for the problem at hand are shown in Table II. This table also shows the bound on TPG for a matching circuit using 7^{th} order Chebyshev topology. The latter are used as the $T_{BF,i}$ in Equation 8.

Since the original Chebyshev filters were designed for 1 dB ripple, initially the ϵ_i's were chosen to be 1 dB for all channels. However, better results were obtained when the values of the ϵ_i's were changed to 10 dB, 3 dB, and 2 dB for Channels 1, 2, and 3, respectively. Table III shows the final component values. There is no special significance in the above ϵ_i values; we include them only for completeness in reporting our calculations. The variation in the values comes about because better convergence is obtained when the lowest frequency channel is allowed the greatest "error"; presumably because the lowest frequency channel also has the greatest fractional bandwidth.

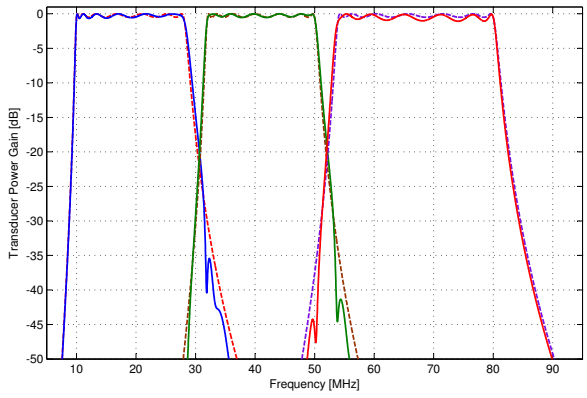

Fig. 4. Performance (TPG) of the initial (50Ω–in, 50Ω–out) multiplexer, assuming constant 50Ω source impedance. Solid lines represent the results when the input port of all multiplexer channels are connected together and dotted lines represent the results when each of the channels are connected with the source separately.

TABLE II
MAXIMUM THEORETICAL TPG CALCULATED FROM BODE–FANO LIMITS ASSUMING BEST FIT RC/RL ANTENNA IMPEDANCES.

Parameter	**Channel–1 (10–28 MHz)**	**Channel–2 (32–50 MHz)**	**Channel–3 (54–80 MHz)**
f_0	16.73 MHz	40 MHz	65.73 MHz
B	110%	40%	50%
R	4.9 Ω	52.5 Ω	674.4 Ω
Series C or L	32.0 pF	191.0 nH	58.2 pF
$\|\Gamma(f_0)\|_{min}$	0.95	4.8×10^{-4}	1.2×10^{-56}
TPG ($n = \infty$)	−10.4 dB	≈ 0 dB	≈ 0 dB
TPG ($n = 7$)	−13.8 dB	≈ 0 dB	≈ 0 dB

The performance results after optimization using standard component values is shown in Figure 5. Note that the optimization significantly improves the performance of Channels 1 and 3. Figure 6 shows γ for various preamplifier noise figures such as 2 dB, 3 dB, and 4 dB. Note that this design achieves large γ (factor of 5 or so) for the worst case of Celestial noise, despite poor TPG, for preamplifier noise figure of 3.0 dB, which is a reasonable noise figure to be achieved using currently available RF devices. We conclude that the design is capable of Celestial noise–dominated sensitivity for all three channels for preamplifier noise figures as high as 4 dB.

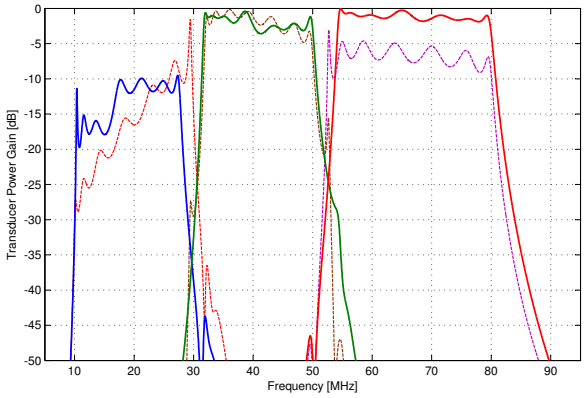

Fig. 5. Performance (TPG) of the multiplexer, assuming simulated impedance of VHF monopole. Solid lines represent the results after optimization and dotted lines represent the results before optimization.

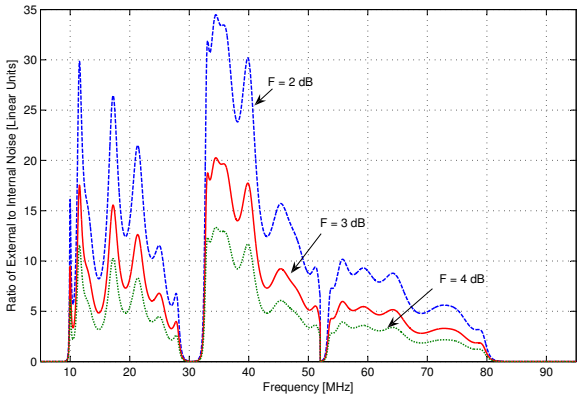

Fig. 6. Performance (γ) of optimized multiplexer for various preamplifier noise figures, assuming only celestial noise.

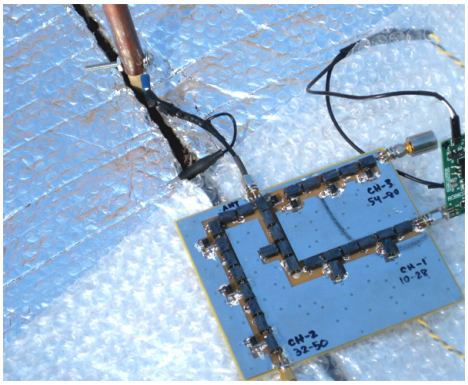

Fig. 7. The multiplexer in the process of field testing.

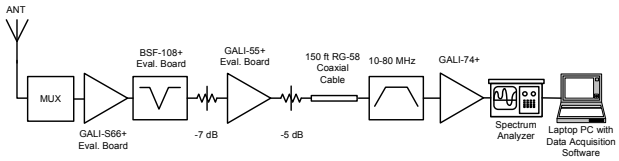

Fig. 8. Block diagram of the field experiment setup. One multiplexer port was tested at a time with the others connected into matched loads. Please visit Mini-Circuits (Inc.) for the detail description of the components shown in the figure [12].

B. Experiment

The optimized multiplexer was implemented and fabricated on a printed circuit board; see [10] for layout and component details. Figure 7 shows the multiplexer board during the field measurement. Figure 8 shows a block diagram of the experiment setup. Figure 9 shows the antenna. This experiment was performed near Blacksburg, VA from 11:00 am to 5:00 pm local time on November 29, 2008.

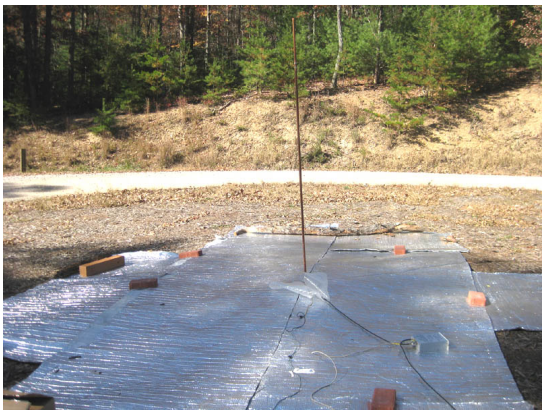

Fig. 9. Antenna and ground screen setup during the field experiment.

We measured PSD at the input of the spectrum analyzer without multiplexer; i.e., $S_{out}^{(1)}$, and also with multiplexer for each channel; i.e., $S_{out}^{(2)}$ (three measurements of $S_{out}^{(2)}$ for three multiplexer channels). From the measurements of $S_{out}^{(1)}$ and $S_{out}^{(2)}$, the TPG for each multiplexer channel is calculated using Equation 6, where the value of noise figure is 2.9 dB (dominated by GALI-74+ amplifier shown in Figure 8), and G_p is the total gain of the signal chain from multiplexer output

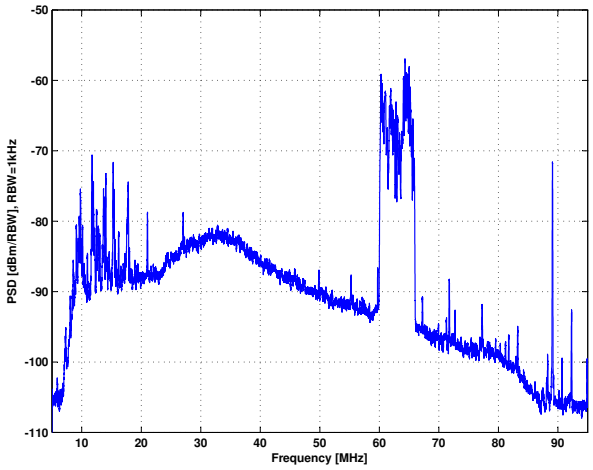

Fig. 10. Measured integrated PSD at the input of spectrum analyzer, averaged over 500 ms with 1 kHz spectral resolution.

to spectrum analyzer input, which ranges between 52 to 44 dB between 10 to 80 MHz (decreasing with increasing frequency).

C. Results

Figure 10 shows $S_{out}^{(1)}$. Note that strong interference is present; in particular, a digital TV station (60–66 MHz) and narrowband HF communications below 20 MHz. To reduce the effect of the interference, we averaged over frequency to reduce the effective resolution to 100 kHz. This greatly mitigates the effect of the HF–band interference, since it exists in a relatively small fraction of the spectral bins. It also reduces the variance of the digital TV spectrum. After frequency averaging, the spectra $S_{out}^{(1)}$ and $S_{out}^{(2)}$ are sufficiently smooth and time–invariant to proceed to calculation of TPG.

Figure 12 shows the resulting measured TPG as well as the predicted TPG. Note the measured performance closely follows the predicted performance, except near the band edges where γ becomes too low for accurate measurement. Within each band, the agreement is sufficiently good that we can conclude that the predictions summarized in Figure 6 are valid; that is, that we are Celestial noise–dominated for preamplifier noise figure as high as 4 dB. Figure 13 shows the TPG of the multiplexer with sharp band-edges. Note that agreement for band edges is limited by the sensitivity of the instrumentation; as shown in Figure 11 and 13, the channel-to-channel isolation is in fact very high.

V. Conclusions

This paper described the use of a *sensitivity–constrained* RF multiplexer to integrate a simple antenna to a receiver with large, multiband tuning ranges. The key idea is to improve bandwidth by allowing the impedance mismatch to degrade in a controlled way such that the sensitivity remains acceptable, and is nominally limited only by external noise. This is effective because at low frequencies where fractional bandwidth tends to be large, high external noise makes impedance matching efficiency less important.

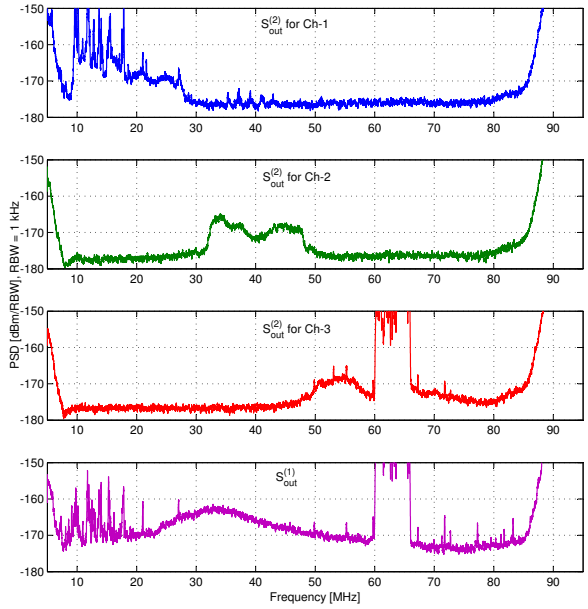

Fig. 11. Measured integrated PSD for each multiplexer channel, and also without the multiplexer. Integrated over 500 ms with 1 kHz spectral resolution. Note that the -177 dBm/kHz noise floor represents the limits of sensitivity of the instrumentation, and thus masks the actual response below this level.

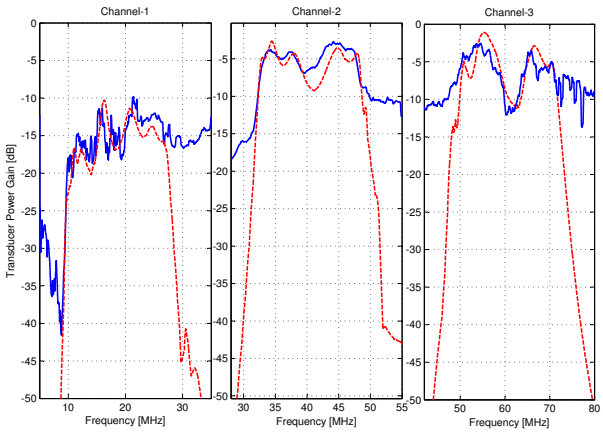

Fig. 12. Performance (TPG) of the multiplexer as built with standard component values. Solid lines represent the measured TPG from the field experiment and dotted lines represent the predicted TPG based on laboratory measurements of the multiplexer's S-parameters.

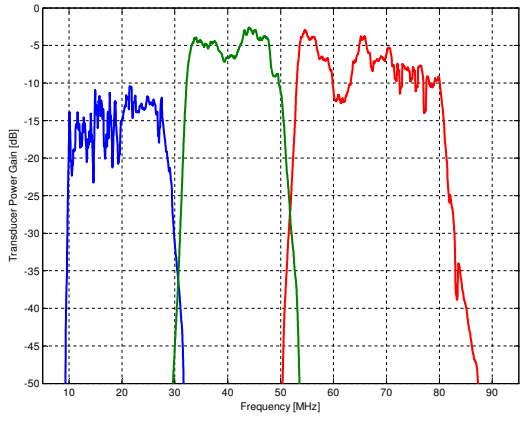

Fig. 13. Performance (TPG) of the multiplexer after (50Ω–in, 50Ω–out) filters presented in Figure 4.

Although the results here are limited to the VHF and low VHF ranges, we have already applied this idea to higher frequency systems. In [10], we designed a system consisting of a commercially-available 418 MHz-resonant monopole combined with a four-channel multiplexer for the frequency ranges 138–174, 220–222, 406–512, and 764–862 MHz, and showed that this system can achieve external noise-limited sensitivity in common noise conditions for front-end amplifier noise figure on the order of 2 dB. However the performance of the implemented hardware is limited in the VHF range by availability of suitable components and parasitic effects from PCB layout.

In this study, no attempt was made to optimize the antenna – the burden was solely on the multiplexer. Antenna–multiplexer co–design (i.e., to design antenna and multiplexer together to achieve jointly optimum performance) should be considered as a possible way to further increase the overall performance.

REFERENCES

[1] S. E. Sussman-Fort and R. M. Rudish, "Non-Foster Impedance Matching of Electrically-Small Antennas," *IEEE Transactions on Antennas and Propagation*, vol. 57, no. 8, pp. 2230–2241, Aug. 2009.

[2] K.-L. Wu and W. Meng, "A Direct Synthesis Approach for Microwave Filters With a Complex Load and Its Application to Direct Diplexer Design," *IEEE Transactions on Microwave Theory and Techniques*, vol. 55, no. 5, pp. 1010–1017, May 2007.

[3] G. Cafaro *et al.*, "A 100 MHz–2.5 GHz Direct Conversion CMOS Transceiver for SDR Applications," in *Proc. IEEE Radio Frequency Integrated Circuits (RFIC) Symposium*, Honolulu, Hawaii, Jun. 2007, pp. 189–192.

[4] R. C.-H. Li, *RF Circuit Design*. Hoboken, NJ: John Wiley & Sons, Inc., 2009.

[5] International Telecommunication Union, "Radio Noise," Tech. Rep. ITU-R P.372-8, 2003.

[6] S. W. Ellingson, J. H. Simonetti, and C. D. Patterson, "Design and Evaluation of an Active Antenna for a 29-47 MHz Radio Telescope Array," *IEEE Transactions on Antennas and Propagation*, vol. 55, no. 3, pp. 826–831, Mar. 2007.

[7] R. M. Fano, "Theoretical Limitations on the Broadband Matching of Arbitrary Impedances," *Journal of Franklin Institute*, vol. 249, Jan–Feb. 1950.

[8] R. W. Rhea, "The Effectiveness of Four Direct Search Optimization Algorithms," *IEEE MTT-S International Microwave Symposium Digest*, vol. 87, no. 2, pp. 697–702, Jun. 1987.

[9] M. M. Weiner, *Monopole Antennas*. Marcel Dekker, 2003.

[10] S. M. Hasan, "New Concepts in Front End Design for Receivers with Large, Multiband Tuning Ranges," Ph.D. dissertation, Virginia Polytechnic Institute and State University, Blacksburg, Virginia, Mar. 2009.

[11] T. H. Cuthbert Jr., *Circuit Design Using Personal Computers*. Malabar, FL: Krieger, 1994.

[12] (2011, May) Mini–Circuits, Inc. [Online]. Available: http://www.minicircuits.com/

PLACE PHOTO HERE

S.M. Shajedul Hasan Biography text here.

PLACE PHOTO HERE

Steven W. Ellingson Biography text here.

TABLE III
ORIGINAL AND NEAREST STANDARD COMPONENT VALUES FOR THE MULTIPLEXER AFTER THE OPTIMIZATION FOR THE SIMULATED IMPEDANCE OF THE VHF MONOPOLE ANTENNA.

Component	**Channel–1**		**Channel–2**		**Channel–3**	
	Original	Standard	Original	Standard	Original	Standard
L1 (nH)	1201.9	1198.0	1179.7	1198.0	1.3	22.0
C1 (pF)	10000.0	10000.0	15.8	15.0	17.1	18.0
L2 (nH)	545.9	538.0	102.2	100.0	41.5	47.0
C2 (pF)	183.9	180.0	152.8	150.0	133.9	120.0
L3 (nH)	1500.0	1498.0	1441.8	1456.0	906.2	960.0
C3 (pF)	54.6	56.0	10.8	10.0	6.3	6.2
L4 (nH)	433.9	538.0	78.2	82.0	35.1	39.0
C4 (pF)	214.8	180.0	204.9	180.0	165.8	150.0
L5 (nH)	1332.9	1336.0	1194.4	1198.0	795.9	784.0
C5 (pF)	64.0	68.0	13.3	12.0	7.3	7.5
L6 (nH)	368.4	380.0	69.7	68.0	34.2	33.0
C6 (pF)	235.9	220.0	231.5	220.0	170.2	180.0
L7 (nH)	753.2	737.0	594.6	538.0	383.8	380.0
C7 (pF)	109.5	120.0	27.3	27.0	15.2	15.0